Journal of Alloys and Compounds 509 (2011) 4295–4299

Contents lists available at ScienceDirect

Journal of Alloys and Compounds

journal homepage: www.elsevier.com/locate/jallcom

Comparative study of ZnO nanostructures grown on silicon (1 0 0) and oxidized porous silicon substrates with and without Au catalyst by chemical vapor transport and condensation

M. Rajabi [a], R.S. Dariani [a,*], A. Iraji Zad [b]

[a] Department of Physics, Alzahra University, Tehran 19938, Iran
[b] Department of Physics, Sharif University of Technology, Tehran 11365, Iran

ARTICLE INFO

Article history:
Received 8 July 2010
Received in revised form 4 January 2011
Accepted 8 January 2011
Available online 15 January 2011

Keywords:
ZnO
Chemical vapor transport and condensation
Nanostructures
Porous silicon
Photoluminescence

ABSTRACT

ZnO tetrapods and rods were grown on silicon and thermally oxidized porous silicon substrates with and without Au catalyst layer by carbothermal reduction of ZnO powder through chemical vapor transport and condensation method (CVTC). Porous silicon was fabricated by electrochemical etching of silicon in HF solution. The effect of substrates on morphology, structure and photoluminescence spectra of ZnO nanostructures has been studied. The texture coefficient (TC) of each sample was calculated from XRD data that demonstrated random orientation of ZnO nanostructures on the oxidized porous silicon substrate. Moreover, TC indicates the effect of Au catalyst layer on formation of more highly oriented ZnO nanorods. The morphology of the samples was investigated by SEM which confirms formation of ZnO nanostructures on oxidized porous silicon substrates with and without catalyst. A blue-green emission has been observed in ZnO nanostructures grown on Si and the oxidized PS substrates without Au catalyst layer by PL measurements.

1. Introduction

In recent years, semiconductor nanostructures have attracted much attention because of their unique properties and their potential applications in electronic and optoelectronic devices. One of the most interesting compound semiconductors is zinc oxide (ZnO). It is a visible transparent metal oxide semiconductor with a direct wide band gap of 3.37 eV and a large exciton binding energy of 60 meV at room temperature which has a diverse group of growth morphologies such as nanowires, nanorods, nanotubes, nanocages, nanobelts and nanocombs. In this group of morphologies, nanowires and nanorods have been widely used in optoelectronic devices such as solar cells [1,2] and photodetectors due to their ability for electron transport [3,4].

In some optoelectronic devices like photoconductors an active material (nanomaterials) should be grown on a proper substrate. Silicon is the most extensive used substrate for growth of one dimensional ZnO nanostructures because of its low cost compared to other substrates such as sapphire. Porous silicon (PS) is another candidate as substrates due to adjustable roughness and structure as well as low price. It can be oxidized easily if we need an insulator substrate [5].

Porous silicon can be fabricated by electrochemical etching of silicon in HF solution. Its room temperature visible photoluminescence (PL) and blue emission which could be understood by presence of nanocrystals or quantum confinement make it a promising material for Si based optoelectronic devices [6]. In addition, it is possible to separate the PS layer from silicon substrate through layer transfer techniques which provide the opportunity to reuse the Si substrate [7].

A variety of methods have been used to grow ZnO nanostructures on such as hydrothermal method [8], sol–gel method [9,10], spray technique [11], magnetron sputtering [12] and vapor phase transport method [13–17]. Moreover, there are few reports on formation of ZnO nanostructures on porous silicon. For example Chang and co-worker investigated growth and characterization of ZnO nanowires grown on porous silicon without using any catalyst [13]. Hsu et al. reported an orientation enhancement for ZnO nanowires with controlled-size porous silicon substrates by vapor–liquid–solid process [14]. Yu et al. studied synthesis, field emission and optical property of different morphology ZnO nanostructures on CuO-catalyzed porous silicon substrates [15–17].

In this paper, we report the growth of ZnO tetrapods and nanorods on Si and oxidized porous silicon with and without catalyst through vapor phase transport method. Morphology and crystal structure of tetrapods and nanorods were studied by XRD and SEM techniques. Then luminescence properties of ZnO nanostructures were studied to investigate effect of the substrate.

* Corresponding author.
E-mail address: sabetdariani@gmail.com (R.S. Dariani).

0925-8388/$ – see front matter © 2011 Elsevier B.V. All rights reserved.
doi:10.1016/j.jallcom.2011.01.041

2. Experiment

In this study we used (1 0 0) oriented, boron doped p-type silicon wafers with resistivity of 1–5 Ω cm and thickness of 525 ± 20 μm. Sample preparation process involved two steps; first, mesoporous silicon formation by electrochemical etching on Si substrates, oxidizing and deposition of Au on some of the PS samples. Second was the growth of ZnO nanowires by vapor phase transport method on the substrates. Electrochemical etching of Si wafer was performed at a constant current density of 20 mA/cm^2 for 20 min in solution of 32% HF (HF:C_2H_5OH = 4:1). Details of the experimental set up and method were reported elsewhere [18]. Oxidation of the porous silicon samples was performed by annealing at 800 °C for 1 h. Au catalyzed samples were prepared by deposition of 5 nm thickness of Au on the silicon and also on the oxidized PS substrates by DC magnetron sputtering. In order to form Au islands the substrates were annealed at 620 ± 10 °C for 30 min.

ZnO tetrapods and rods were grown in a horizontal quartz tube furnace. One side of quartz tube was connected to gas inlet and the other side was connected to environment. The distance between the gas inlet and the center of quartz boat was about 55 cm. A source material, which was a mixture of zinc oxide (99.99%, Merck) and graphite powders (99.99%, LOBA chemie) with equal weight ratio were placed into a small quartz tube (2.7 cm inner diameter and 20 cm length). Similar substrates were placed at different distances from the source material downstream along the direction of gas flow which was resulted in different substrate temperatures due to the natural temperature gradient along the furnace. The small quartz tube was transferred into the outer quartz tube (3.8 cm inner diameter and 95 cm length) of horizontal furnace. The source material which was placed at the central hot zone of the furnace was heated to 990 °C at a rate of 20 °C/min and was kept at this temperature for 1 h under constant flow of high purity nitrogen gas at a rate of 500 sccm (standard cubic centimeters per minutes). Then, the furnace was cooled down to room temperature naturally. Under these conditions the substrates temperature during growth process were determined to be in the range of 830–930 °C. The surface color of samples grown on both Si and oxidized PS substrates were white and the samples grown on Si and oxidized PS with catalyst appeared gray and violet, respectively.

Table 1
The calculated values lattice constants.

Substrate	a (Å)	c (Å)
Si (1 0 0)	3.2535	5.1992
oxidized PS	3.2537	5.2094
Au catalyzed Si	3.2513	5.2053
Au catalyzed oxidized PS	3.2531	5.2051

The crystal structure and surface morphology of ZnO nanowires were characterized by X-ray diffraction (XRD) with Cu Kα radiation, scanning electron microscope (SEM, Philips XL30) and atomic force microscope (AFM; Veeco-Termo Microscopes) in contact mode. The photoluminescence measurements were made at room temperature using a UV lamp and a filter centered at a wavelength of 254 nm and UV–visible (Avantes-2048Tec) Spectrometer.

3. Results and discussion

To study the effect of substrate on crystal structure we performed XRD experiments on the samples. Fig. 1(a)–(d) shows diffraction pattern of ZnO grown on Si, oxidized PS, Au catalyzed Si and PS. All the diffraction peaks in the spectra could be indexed to the hexagonal-wurtzite structure of ZnO. The ZnO nanostructures grown on oxidized PS (Fig. 1(b)) exhibit regular crystallographic pattern of bulk material. Table 1 presents the lattice constants of each sample were calculated from XRD patterns which are in good agreement with the standard data a = 3.2539 Å and c = 5.2098 Å (JCPDS card 80-0075) especially for the structures grown on oxi-

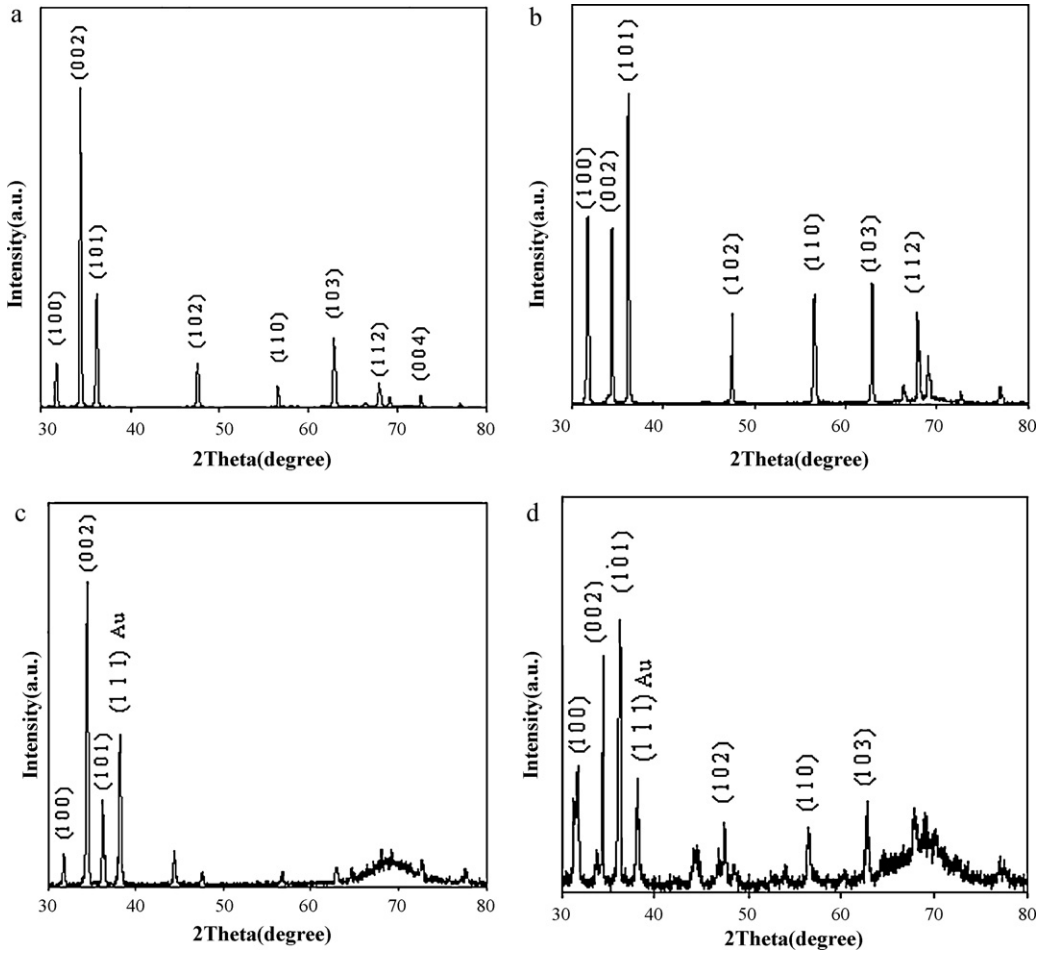

Fig. 1. X-ray diffraction of ZnO nanostructures deposited under same growth conditions on (a) Si substrate, (b) oxidized PS substrate, (c) Si substrate with Au catalyst, and (d) oxidized PS substrate with Au catalyst.

Table 2
The values of TC calculated for three higher diffraction peaks.

	Si	Au catalyzed Si	Oxidized PS	Au catalyzed PS oxide
TC (1 0 0)	0.18	0.32	0.83	0.76
TC (0 0 2)	2.10	3.40	0.99	1.56
TC (1 0 1)	0.34	0.40	0.74	0.96

Table 3
The values of root mean square roughness and mean height of Si and oxidized porous silicon.

	RMS roughness (nm)	Mean height (nm)
Si (1 0 0)	0.40	2.44
Oxidized porous silicon	19.12	176.4

dized PS with and without Au catalyst (Fig. 1(b) and (d)), within experimental error. Except Au and SiO_2 peaks no diffraction peaks from impurities like Zn were detected in these samples. Also the strong intensity of ZnO diffraction peaks indicates that the resulting products have high purity of ZnO. Comparing the intensity of SiO_2 related peak (around 21.8°) of ZnO structures grown on Si and oxidized porous silicon substrates shows higher amount of SiO_2 on the oxidized PS than Si substrates. The weak oxide peak in the XRD spectrum of Si substrate is related to silicon native oxide and thin oxide growth during CVTC process before nucleation of ZnO structures.

The relative intensities of three dominant characteristic peaks at (1 0 0) (0 0 2) and (1 0 1) show some differences for different samples. In Fig. 1(a) and (c) the high diffraction peak at (0 0 2) plane shows preferred orientation along this direction. The comparison of observed pattern in Fig. 1(b) for ZnO grown on oxidized PS and standard pattern dose not show any preferred orientation for this sample. To determine the preferred orientation of structures grown on oxidized PS with Au catalyst (Fig. 1(d)), the texture coefficient of three higher diffraction peaks at (1 0 0), (0 0 2) and (1 0 1) of this and other samples were calculated and listed in Table 2. Texture coefficient (TC) determines the orientation of the ZnO nanostructures. The texture coefficient of (h k l) plane (TC (h k l)) can be calculated using the following expression [14]:

$$\mathrm{TC(h\,k\,l)} = \frac{I_{(\mathrm{h\,k\,l})}/I_{\mathrm{o(h\,k\,l)}}}{N^{-1}\sum_N I_{(\mathrm{h\,k\,l})}/I_{\mathrm{o(h\,k\,l)}}} \quad (1)$$

where $I_{(\mathrm{h\,k\,l})}$ is the measured intensity, $I_{\mathrm{o(h\,k\,l)}}$ is the standard intensity of (h k l) plane taken from the JCPDS data, and N is the total number of diffraction peaks. For a sample with randomly oriented crystallite TC (h k l) is equal to 1. When this value is larger than 1 a preferred orientation exists along the (h k l) plane. Generally, the preferred growth direction of ZnO nanostructures is [0 0 2]. The data are presented in Table 2 confirms the randomly orientation of ZnO nanostructures grown on our oxidized PS (Fig. 1(b)). Also, the value of 1.56 for TC (0 0 2) implies the preferred orientation of rod shape along this direction on oxidized PS substrate with Au catalyst.

To check the above results and observe surface morphology of the samples we performed SEM and AFM experiments. Fig. 2 shows the surface morphology and distribution of Au islands on Si and oxidized PS substrates after annealing. Concentration and shape of Au islands on the oxidized PS substrates is larger and more irregular than on Si. Different Au structures are due to lower surface roughness of Si substrate that provides higher surface diffusion for Au adatoms and more spheres like island. Fig. 3 shows three dimensional AFM images of silicon and oxidized PS for a scanning area of 5 μm × 5 μm. Surface roughness and mean height of both surfaces were measured and are illustrated in Table 3. In fact rougher surface produce higher Au island density and provide more nucleation center for ZnO wires. This causes stronger adhesion of ZnO layer to the PS substrate as we will discuss later [14].

Fig. 4 shows SEM images of ZnO nanowires grown on silicon (Fig. 4(a)) and oxidized PS (Fig. 4(b)) substrates without Au catalyst. Data shows that growth of ZnO nanowires is possible on oxidized PS substrate without catalyst. But, there are some differences in the detailed geometrical morphologies of rods grown on these two different substrates. The ZnO wires synthesized on silicon substrate without catalyst have a uniform diameter over their entire length and a hexagonal shape as shown in inset image of Fig. 4(a) unlike the structure of wires in Fig. 4(b). The random orientation and irregular shapes of the rods grown on top of oxidized porous layer may be related to rough surface and rather thick SiO_2 layer on oxidized PS substrates. The diameter of ZnO nanowires on both substrates is in the range of 200–900 nm and their length in the range of 5–10 μm. Fig. 5 shows SEM images of ZnO wires grown on Au catalyzed silicon (Fig. 5(a)) and oxidized porous Si substrates (Fig. 5(b) and (c)). Au catalyst could decrease aspect ratio of the wires due to larger rod's diameter around 0.3 μm and reduces the rod's density on the oxidized PS surface. In fact lower XRD signal/noise ratio and wider peak around 70° may be due to interface formation of silicon oxide and ZnO as we can observe in Fig. 5(b). Long ZnO wires in (0 0 2) direction as we expected from XRD is shown in Fig. 5(b)

ZnO is a luminescent material. Usually two emission bands are observed in photoluminescence spectrum, a visible blue-green band related to deep level defects, such as oxygen or Zn vacancies and Zn interstitials, and a narrow UV emission in a range of 370–390 nm due to exciton recombination near band edge [19–21]. It has been suggested that these two emission bands are in competition with each other and the high crystallinity of structure enhances the UV emission. Fig. 6 shows the room temperature PL spectra of ZnO tetrapods and rods grown on Si (Fig. 6(a)) and

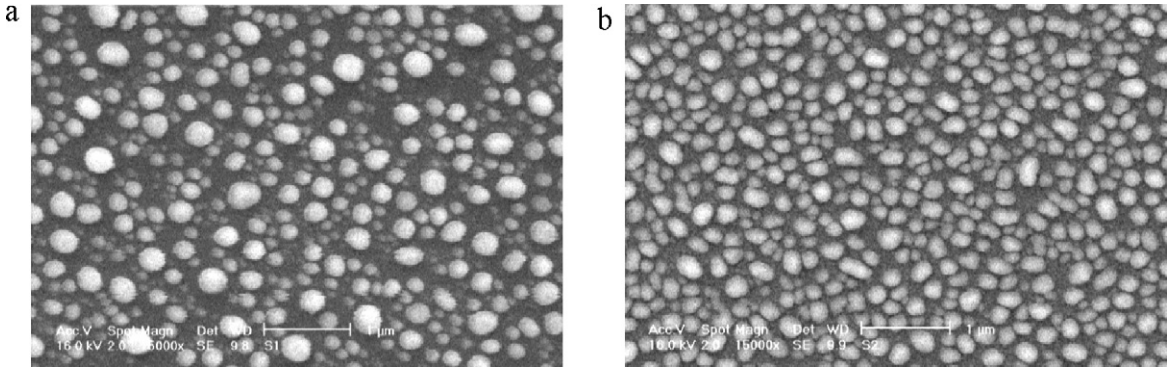

Fig. 2. SEM images of Au layer on (a) Si and (b) oxidized PS after annealing.

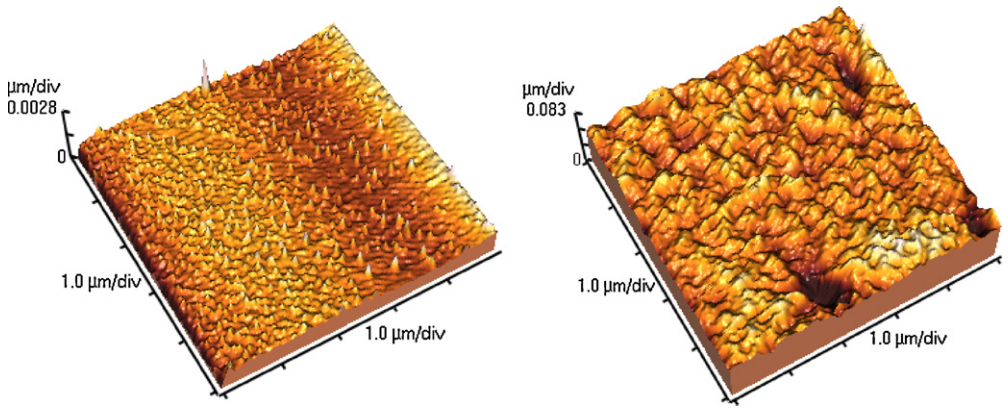

Fig. 3. Three dimensional AFM images of (a) silicon and (b) oxidized PS surfaces.

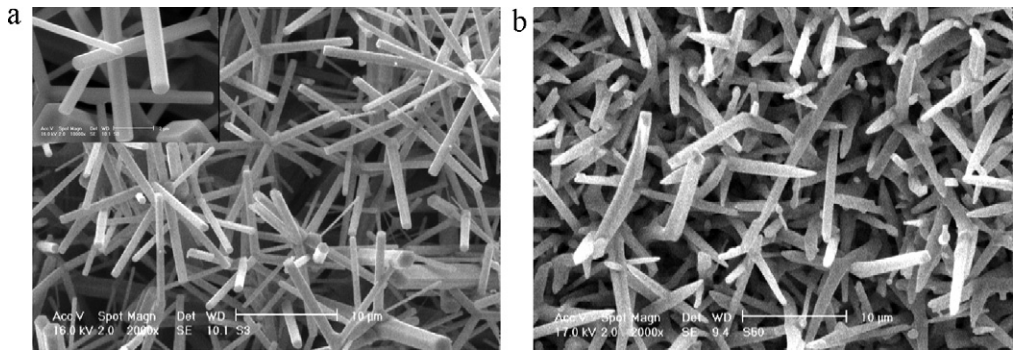

Fig. 4. SEM images of ZnO tetrapods and rods grown on (a) a silicon substrate and (b) an oxidized PS substrate without Au catalyst under same magnification. The inset picture in (a) has a higher magnification with a scale bar of 2 µm to show hexagonal shape wires formed on Si substrate.

oxidized PS (Fig. 6(b)) without any catalyst. The nanostructures grown on Au catalyzed substrates did not present any detectable luminescence. These spectra consist of a very weak UV emission peak at ~390 nm compare to strong blue and green emission bands centered at around 490 nm and 545 nm, respectively. The origin of visible emission bands related to deep level defects emission has not been conclusively established [19]. A proposed hypothesis relates visible emission band around 495 nm to oxygen vacancy and emission peak ~540 nm to V_0^{**} [22,23]. The weaker blue-green emission of ZnO rods grown on oxidized PS might be related to the lower oxygen vacancies concentration in ZnO rods compared to structures grown on Si. Roy et al. [24] studied luminescence proper-

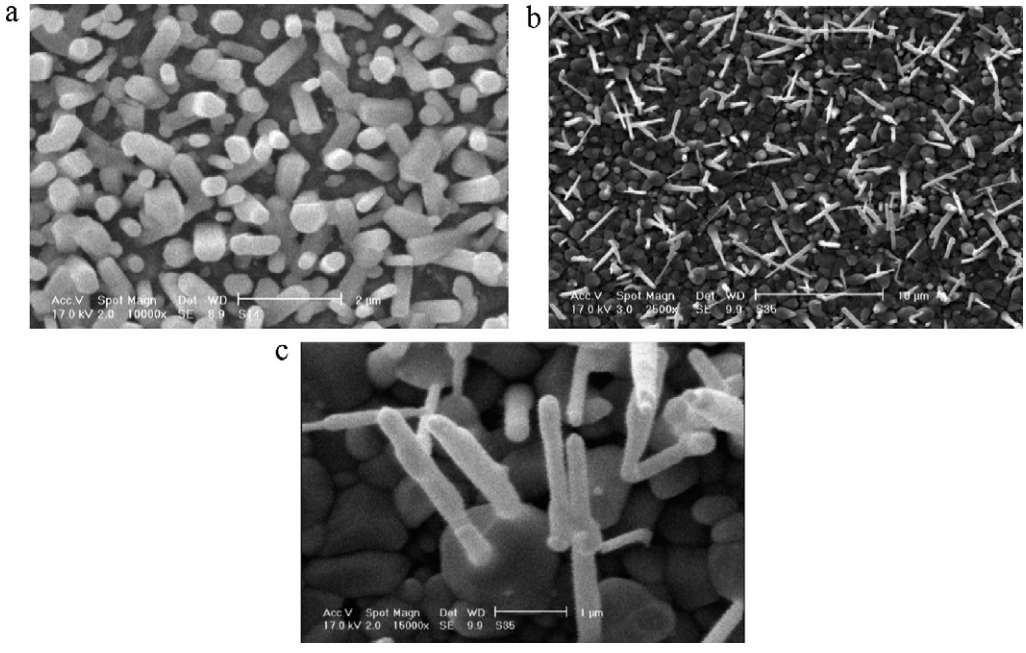

Fig. 5. SEM images of ZnO nanowires grown on Au catalyzed (a), silicon (b), and (c) oxidized PS substrates with different magnifications.

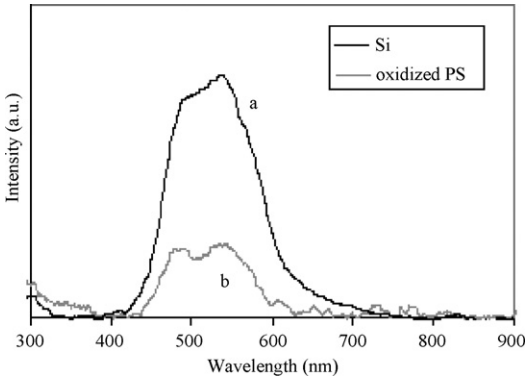

Fig. 6. Room temperature PL spectra of ZnO structures grown on (a) Si and (b) oxidized PS substrates.

ties of ZnO nanostructures under different gas flows. They reported the similar result due to nitrogen impurity for ZnO tetrapods which have been grown by thermal evaporation of Zn under dry nitrogen flow. As we mentioned Au catalyzed samples did not show PL perhaps due to high defects and thin ZnO layer. Also, this quenching of PL could be a result of structural defects as proposed by Sieber et al. [25]. More study is in progress to understand the origin of the observed PL spectra.

It is known that nucleation as the first stage of growth process has an important effect on shape, size and alignment of ZnO structures. The morphology of substrate surface has influenced the growth process via this stage. For the growth process without Au catalyst the Zn vapor produced by carbothermal reduction of ZnO powder is transported and condensed on substrates at lower temperatures. The oxidation of liquid Zn on substrates forms ZnO nuclei. Then, the tetrapods and rods grow through vapor solid mechanism. The shape and size of nuclei could control structure of the final rods.

The growth process in the presence of Au catalyst can be governed by vapor liquid solid mechanism. Comparing the diameter of Au islands on Si substrate and diameter of ZnO nanostructures grown on them can be an evidence for VLS mechanism. Although, the Au particles may either be at the root or tips of nanorods [26]. The growth process on Au catalyzed oxidized porous silicon is a little different because of higher surface roughness of oxidized PS layer which leads to non-spherical shape of Au islands on it. So, Au islands act as nucleation sites for growth of ZnO particles. Then nanorods nucleate on surface facets and boundaries of these particles.

4. Conclusions

Randomly oriented ZnO rods were grown on oxidized porous silicon substrate by carbothermal reduction of ZnO. The texture coefficient calculated from XRD data shows that the orientation of ZnO nanorods grown on oxidized porous layer with Au catalyst is along (0 0 2) and indicates the effect of catalyst on growth process. We compared the structure and morphology of ZnO nanostructures grown on oxidized porous silicon substrate with nanostructures formed on silicon substrate.

References

[1] Y.F. Hsu, Y.Y. Xi, A.B. Djurisic, W.K. Chan, Appl. Phys. Lett. 92 (2008) 133507–133509.
[2] J.B. Baxter, E.S. Aydil, Appl. Phys. Lett. 86 (2005) 053114–053116.
[3] K.J. Chen, F.Y. Hung, S.J. Chang, S.J. Young, J. Alloys Compd. 479 (2009) 674–677.
[4] H. Zhou, G. Fang, L. Yuan, C. Wang, X. Yang, H. Huang, C. Zhou, X. Zhao, Appl. Phys. Lett. 94 (2009) 013503–013505.
[5] C. Soci, A. Zhang, B. Xiang, S.A. Dayeh, D.P. Dayeh, D.P.R. Alpin, J. Park, X.Y. Bao, Y.H. Lo, D. Wang, Nano Lett. 7 (4) (2007) 1003–1009.
[6] L.T. Canham, Appl. Phys. Lett. 57 (1990) 1046–1048.
[7] C.S. Solanki, R.R. Bilyalov, J. Poortmans, J. Nijs, R. Mertens, Sol. Energy Mater. Sol. Cells 83 (2004) 101–113.
[8] J.P. Kar, M.H. Ham, S.W. Lee, J.M. Myoung, Appl. Phys. Lett. 255 (2009) 4087–4092.
[9] R.G. Singh, F. Singh, V. Agarwal, R.M. Mehra, J. Phys. D: Appl. Phys. 40 (2007) 3090–3093.
[10] C. Shaoqiang, Z. Jian, F. Xiao, W. Xiahua, L. Laiqiang, S. Yanling, X. Qingsong, W. Chang, Z. Jianzhong, Z. Ziqiang, Appl. Surf. Sci. 241 (2005) 384–391.
[11] H. Elhouichet, M. Oueslati, Mater. Sci. Eng. B 79 (2001) 27–30.
[12] P. Prabarkaran, M. Peres, T. Monteiro, E. Fortunato, R. Martins, I. Ferreira, J. Non-Cryst. Solids 345 (2008) 2181–2185.
[13] C.C. Chang, C.S. Chang, Jpn. J. Appl. Phys. 43 (2004) 8360–8364.
[14] H.C. Hsu, C.S. Cheng, C.C. Chang, S. Yang, C.S. Chang, W.F. Hsieh, Nanotechnology 16 (2005) 297–301.
[15] K. Yu, Y. Zhang, L. Luo, S. Ouyang, H. Geng, Z. Zhu, Mater. Lett. 59 (2005) 3525–3529.
[16] K. Yu, Y. Zhang, L. Luo, W. Wang, Z. Zhu, J. Wang, Y. Cui, H. Ma, W. Lu, Appl. Phys. A 79 (2004) 443–446.
[17] K. Yu, Y. Zhang, R. Xu, D. Jiang, L. Luo, Q. Li, Z. Zhu, W. Lu, Solid State Commun. 133 (2005) 43–47.
[18] M. Rajabi, R.S. Dariani, J. Porous Mater. 16 (2009) 513–519.
[19] A.B. Djurisic, Y.H. Leung, Small 2 (2006) 944–961.
[20] H. Liu, G. Piret, B. Sieber, J. Laureyns, P. Roussel, W. Xu, R. Boukherroub, S. Szunerits, Electrochem. Commun. 11 (2009) 945–949.
[21] B. Sieber, H. Liu, G. Piret, J. Laureyns, P. Roussel, B. Gelloz, S. Szunerits, R. Boukherroub, J. Phys. Chem. C 113 (2009) 13643–13650.
[22] M.K. Patra, K. Manzoor, M. Manoth, S.P. Vadera, N. Kumar, J. Lumin. 128 (2008) 267–272.
[23] A. van Dijken, E.A. Meulenkamp, D. Vanmaekelbergh, A. Meijerink, J. Phys. Chem. B 104 (2000) 1715–1723.
[24] V.A.L. Roy, A.B. Djurisic, W.K. Chan, J. Gao, H.F. Lui, C. Surya, Appl. Phys. Lett. 83 (2003) 141–143.
[25] B. Sieber, A. Addad, S. Szunerits, R. Boukherroub, J. Phys. Chem. Lett. 1 (2010) 3033–3038.
[26] K.W. Kolanski, Curr. Opin. Solid State Mater. Sci. 10 (2006) 182–191.